A&A manuscript no.
(will be inserted by hand later)

Your thesaurus codes are:
03 (10.03.1; 11.01.2; 11.10.1; 13.25.2; 02.01.2; 02.02.1)

ASTRONOMY AND ASTROPHYSICS
February 5, 2001

The jet model for Sgr A*: radio and X-ray spectrum

Heino Falcke and Sera Markoff[1]

Max-Planck-Institut für Radioastronomie, Auf dem Hügel 69, 53121 Bonn, Germany (hfalcke,smarkoff@mpifr-bonn.mpg.de)

Astronomy & Astrophysics, Vol. 362, p. 113 (2000)

Abstract. The preliminary detection of the Galactic Center black hole Sgr A* in X-rays by the Chandra mission, as well as recent mm-VLBI measurements, impose strict constraints on this source. Using a relativistic jet model for Sgr A*, we calculate the synchrotron and synchrotron self-Compton emission. The predicted spectrum provides an excellent fit to the radio spectrum and the the X-ray observations. Limits on the infrared flux and the low X-ray flux require a high-energy cut-off in the electron spectrum at $\gamma_{\rm e} \lesssim 100$. The implied lack of a significant power-law tail of high-energy electrons also suppresses the appearance of the extended, optically thin radio emission usually seen in astrophysical jets. The jet therefore appears rather compact and naturally satisfies current VLBI limits. The initial parameters of the model are tightly constrained by the radio spectrum and the "submm-bump" in particular. While the jet most likely is coupled to some kind of accretion flow, we suggest that the most visible signatures can be produced by this outflow. If SSC emission from the jet contributes to the Sgr A* spectrum, significant variability in X-rays would be expected. The model could be generic for other low-luminosity AGN or even X-ray binaries.

Key words: Galaxy: center – galaxies: active – galaxies: jets – X-rays: galaxies – accretion – black hole physics

1. Introduction

Sagittarius A* (Sgr A*) is the compact radio source at the Galactic Center, which mounting evidence suggests is the signature emission of a supermassive black hole. Proper motion studies with radio interferometers (Reid et al., 1999; Backer and Sramek, 1999) place Sgr A* at the apparent dynamical center of the Galaxy, with a lower limit on its mass of $\sim 10^3 M_\odot$. Similarly the motions of the surrounding stars, as well as near-infrared (NIR) line spectroscopy, indicate a mass of $2.6 \cdot 10^6 M_\odot$ enclosed within ~ 0.01 pc (Haller et al., 1996; Eckart and Genzel, 1996; Ghez et al., 1998). These measurements rule out any known multiple star system.

At the same time, Very Long Baseline Interferometry (VLBI) places strict upper limits on the frequency-dependent size and structure of Sgr A*. Observations at 86 & 220 GHz (Rogers et al., 1994; Krichbaum et al., 1998) constrain Sgr A* to be around 0.06-0.2 milli-arcseconds (mas) at these frequencies.

The radio spectrum of Sgr A* is slightly inverted with a "submm-bump" and a steep cut-off towards the IR (e.g., Serabyn et al. 1997, Falcke et al. 1998), while the radio flux is variable on scales of weeks to months (e.g., Wright & Backer 1993, Falcke 1999b). Sgr A* also shows an unusually high ratio of circular to linear polarization (Bower et al., 1999b).

The latest information comes from the detection of Sgr A* with the X-ray satellite Chandra (Baganoff et al., 1999; Baganoff et al., 2001). The first epoch data show a point source at the location of Sgr A* with an X-ray luminosity roughly two times below the earlier ROSAT limit (Predehl and Trümper, 1994) and a photon index of $\sim 2.75^{+1.25}_{-1.00}$. This new measurement provides a crucial constraint for any model of radiative emission from Sgr A*.

While all current models for Sgr A*'s radio emission consider accretion onto the black hole as the driving force, they separate into two generic classifications. In models proposed by, e.g., Rees (1982), Melia (1992), and Narayan et al. (1995), the radio emission is produced by processes in the accretion flow itself. Alternatively, Falcke et al. (1993) propose that the radio emission stems from an outflow (see also Reynolds & McKee 1980) originating in the accretion disk.

One currently popular accretion model is the Advection-Dominated Accretion Flow (ADAF; Narayan et al. 1995). While it may explain the faintness of optical and ultra-violet (UV) emission, its application to explain the compact radio emission from low-luminosity AGN (LLAGN) is problematic. For instance, in two well-known LLAGN with radio nuclei similar to Sgr A*, M81 (Bietenholz et al., 2000) and NGC 4258 (Herrnstein et al.,

Send offprint requests to: hfalcke@mpifr-bonn.mpg.de
[1] Alexander-von-Humboldt research fellow

1998), intense observations with VLBI revealed core-jet structures but found no evidence for radio emission from an ADAF. Furthermore, a systematic survey of LLAGN with the VLA and the VLBA (Nagar et al., 2000; Falcke et al., 2000b) found many compact radio nuclei, none of which show the highly inverted spectrum expected in the ADAF model. On the other hand, the rather flat radio spectra found are quite naturally explained within jet models. For Sgr A* itself, the standard ADAF model falls short of explaining the cm-wave radio emission by more than an order of magnitude and additional assumptions must be imposed in order to match the spectrum (Mahadevan, 1998; Özel et al., 2000).

The difference in spectral index between a jet and an ADAF model stems from the fact that in the latter the energy of the radiating particles (i.e. temperature) is a function of radius due to the dissipation of energy in the viscous accretion flow, while an unperturbed supersonic jet is to first order dissipationless and quasi-isothermal. We mean this in the sense that there is only limited cooling, due to adiabatic losses which result from the longitudinal pressure gradient (see Eq. 2). Hence, the relative spectral indices reflect the fundamentally different concepts underlying these models.

Given these issues, it would seem timely to revisit the jet model with the additional constraints provided by the Chandra observations, especially as Lo et al. (1998) have claimed the first tentative evidence for a jet structure in Sgr A* from 7 mm VLBI. Here, we present a numerical calculation of the jet model using more realistic electron distributions and the contribution of synchrotron self-Compton (SSC) emission. We note that the low X-ray fluxes detected by Chandra were in fact expected in models invoking SSC emission (e.g., Beckert & Duschl 1997) and predicted for the jet model (Falcke, 1999a).

2. The Jet Model

The basic model was already described in detail in Falcke (1996a). Symmetrically on either side of the accretion flow a magnetized, relativistic proton and electron plasma (adiabatic index $\Gamma = 4/3$) is ejected from a nozzle where it becomes supersonic, with an initial sound speed (in units of the speed of light c) of $\beta_{\rm s,0} = \sqrt{(\Gamma-1)/(\Gamma+1)} \sim 0.4$. Each jet accelerates along its axis through its pressure gradient and expands sideways with its initial sound speed. The velocity field with bulk Lorenz factor $\gamma_{\rm j}$ is then given by the Euler equation (see Eq. 1 in Falcke 1996a)

$$\frac{\partial \gamma_{\rm j}\beta_{\rm j}}{\partial z}\left(\frac{\left(\frac{\Gamma+\xi}{\Gamma-1}\right)(\gamma_{\rm j}\beta_{\rm j})^2-\Gamma}{\gamma_{\rm j}\beta_{\rm j}}\right)=\frac{2}{z} \quad (1)$$

with $\xi = (\gamma_{\rm j}\beta_{\rm j}/(\Gamma(\Gamma-1)/(\Gamma+1)))^{1-\Gamma}$. As before, the gravitational potential is ignored since its influence is rather small in the supersonic regime considered here. The size of the nozzle z_0, i.e. the location of the sonic point, remains a free parameter, since the exact launching mechanism for astrophysical jets is unknown.

Given an initial magnetic field B_0, a relativistic electron total number density n_0 with a characteristic electron energy $\gamma_{\rm e,0} m_{\rm e} c^2$, the radius r_0 of the nozzle, and taking only adiabatic cooling due to the longitudinal pressure gradient (i.e. $\propto \mathcal{M}^{\Gamma-1}$, where $\mathcal{M}$ is the Mach number) and dilution by the lateral expansion into account, one can determine the magnetic field $B(z_*)$, particle density $n(z_*)$, electron Lorentz factor $\gamma_{\rm e,0}(z_*)$, and jet radius as a function of the dimensionless distance from the nozzle $z_* = (z-z_0)/r_0$:

$$\begin{aligned}
&\mathcal{M}(z_*)=\frac{\gamma_{\rm j}\beta_{\rm j}}{\gamma_{\rm s,0}\beta_{\rm s,0}},\ n(z_*)=n_0\cdot(r(z_*)/r_0)^{-2}\,\mathcal{M}^{-1}(z_*),\\
&r(z_*)=r_0+z_*/\mathcal{M}(z_*),\ \gamma_{\rm e}(z_*)=\gamma_{\rm e,0}\cdot\mathcal{M}^{-1/3}(z_*),\\
&B(z_*)=B_0\cdot(r(z_*)/r_0)^{-1}\,\mathcal{M}^{-2/3}(z_*). \quad (2)
\end{aligned}$$

This fixes the basic parameters for synchrotron and SSC emission along the entire jet.

By approximating the jets as a series of cylindrical sections, we can calculate the total emission by integrating over the contributions from each component. For each segment the optical depth to synchrotron absorption is $\tau_\nu = \frac{\pi}{2}\alpha_\nu r(z_*)/D\sin\theta_i$, where θ_i is the angle between the jet axis and the line of sight, α_ν is the absorption coefficient, $D=[\gamma(1-\beta\cos\theta_i)]^{-1}$ is the Doppler factor accounting for the angle aberration (e.g., Lind & Blandford 1985) due to the relativistic bulk velocity, $\beta(z_*)c$, in the jet. Using the transfer equation for source-only emission, assumed constant within the segment, $I_\nu(\tau_\nu)=(1-{\rm e}^{-\tau_\nu})S_\nu$ where $S_\nu = j_\nu/\alpha$ is the source function. Assuming isotropic emission in the rest frame of the cylindrical shell, the net flux out of the component is thus $F_\nu = 4\pi I_\nu$. The observed flux density is then $F'_{\nu'} = D^2 2r(D\sin\theta_i)\Delta z F_\nu/4\pi d_{\rm gc}^2$, where the distance to the Galactic Center is assumed to be $d_{\rm gc} = 8.5$ kpc and the $2r(D\sin\theta_i)\Delta z$ factor is the approximate projected surface area of the radiating cylinder. In the limits of $\tau\to 0$ and $\tau\to\infty$ we recover the correct optically thin and optically thick solutions.

To calculate the inverse-Compton up-scattered emission for the same segment, we can ignore projection effects since the optical depth for Compton scattering is small and use the self-absorbed synchrotron emission in the component frame calculated above. Then, using the general expression for Compton scattering (e.g., Blumenthal & Gould 1970) by a distribution of relativistic electrons (including the Klein-Nishina limit), we find the SSC emission in the frame of the component which then is transformed into the observer's frame as before.

Relativistic beaming and possible – but model-dependent and difficult to quantify – absorption in an accretion flow limit the visibility of the second jet pointing away from Earth (see, e.g., the faint counter-jet in the almost edge-on disk of NGC4258; Herrnstein et al. 1998). For simplicity the counter jet is therefore ignored in our calculations. The most noticeable effect of this jet for the range of parameters discussed here ($\theta_i \sim 50°$, $\gamma_{\rm j}\beta_{\rm j} = 0.4 - 3$) could be a $\leq 30\%$ increase in flux density at the highest frequencies from the brighter nozzle component, quickly dropping to 10% and less in the mm-wave range. We point out that we also ignore here – as with all other current models for Sgr A* – any general relativistic effects on the spectrum and the emission region (see Falcke et al. 2000a). Thus, possible corrections due to the counter-jet and the light propagation in the Kerr metric have to be absorbed by the other parameters in the model. Given the overall simplicity of the model we feel this is justified.

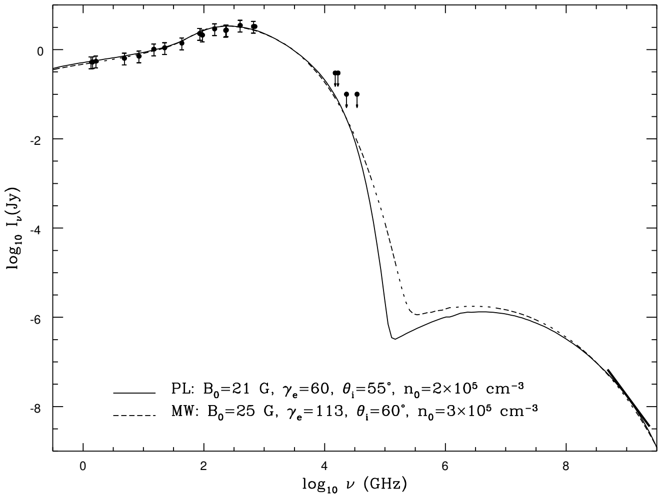

Fig. 1. Broad-band spectrum of Sgr A*. The dots are the simultaneous spectrum measured by Falcke et al. (1998) with additional high-frequency data discussed by Serabyn et al. (1997). We have added 10% errors for typical short-term variability. This is quite conservative—from a theorists point of view, as Sgr A* is known to vary up to 30-100% during flares (Zhao et al., 2001; Tsuboi et al., 1999), and we have not accounted for systematic errors in the mm-range. In the hard X-rays we show the possible detection of Sgr A* with Chandra in the range 2-10 keV which is relatively unaffected by absorption (Baganoff et al., 2001). We show our model spectrum for a power-law distribution of electrons (PL) and a relativistic Maxwellian distribution (MW). The radius of the nozzle is $r_0 \approx 4R_{\rm s}$, while its height is $z_0 \approx 2r_0$.

3. Results

3.1. Radio Spectrum

In theory, this model has six free parameters: the radius of the nozzle, r_0, the location of the sonic point (corresponding to the length of the nozzle),z_0, the magnetic field, B_0, the equipartition factor, k (which determines the electron density n_0), the inclination angle, θ_i, and the characteristic Lorentz factor of the electron distribution, $\gamma_{\rm e,0}$. In earlier papers (e.g., Falcke et al. 1993) we used the jet-disk coupling to determine some of these parameters, however, most parameters are in fact well-constrained by data or obvious physical arguments.

Firstly, the radius of the nozzle cannot be any smaller than the event horizon of the black hole, while the above mentioned VLBI observations provide an upper limit of $\lesssim 15$ Schwarzschild radii. The same is true for the sonic point and nozzle height z_0 — indeed the final solution can be obtained with a symmetric nozzle, i.e. $z_0 \sim 2r_0$. In addition, as shown in Falcke (1996b), observed the high- and low-frequency turnover as well as the peak flux of the submm-bump directly determine the magnetic field, electron Lorentz factor, and density in the nozzle region subject only to uncertainties in the measured spectrum. Fitting the submm-bump with the additional constraint of an equipartition solution, therefore limits the number of entirely "free" parameters to one, i.e. the inclination angle θ_i. Of course, the most likely inclination angle for a randomly oriented source is around 57° and very small or very large values for θ_i appear unlikely but are also not completely excluded.

Furthermore, a steep cut-off or highly peaked electron distribution is necessitated by the stringent IR upper limits. Consequently, we see no optically thin high-frequency emission as exists, for example, in blazars, which would be due to a power-law tail of high-energy electrons.

Here, we explore two possibilities for common astrophysical electron distributions. First, we consider a narrow power-law with a standard energy index $p = 2$ and a sharp cut-off at roughly $5\gamma_{\rm e,0}$. We also consider a relativistic thermal Maxwellian distribution with $\gamma_{\rm e,0} \approx 3.5\frac{kT}{m_e c^2}$. An alternative energy distribution, i.e. one which is produced via hadronic processes, will be explored in a later paper (Markoff et al., 2000). However, the basic results remain rather unchanged as long as the distribution is relatively narrow.

Fig. 1 shows the best fits to the submm- and cm-wave radio spectrum for the two electron distributions under the condition of equipartition, with nozzle parameters given in the plots. We show F_ν rather than νF_ν because it is more conducive for judging the quality of the spectral fit at cm-waves. The nozzle component accounts for most of the submm-bump, as well as the main Compton component, and the low-frequency spectrum stems from the emission of the more distant parts along the jet. Within the model, the slope of the cm-wave spectrum and the ratio between cm- and submm-emission is mainly determined by the inclination angle. The parameters we obtain for the jet and nozzle are close to those used by Falcke (1996b), Beckert & Duschl (1997), Falcke & Biermann (1999).

3.2. X-ray flux

Once the radio spectrum due to synchrotron emission is fixed, so is the Compton up-scattered spectrum. The peak frequency of the latter is $\sim 4\gamma_{\rm e,0}^2$ times the peak frequency

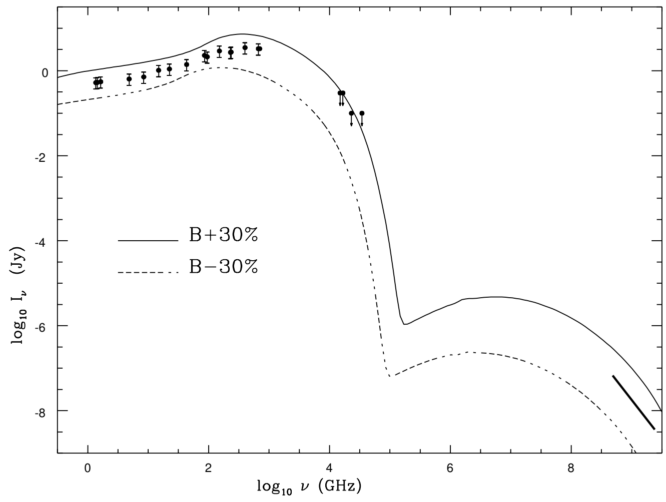

Fig. 2. Same as the power-law curve in Fig. 1, with the magnetic field plotted for values 30% higher (solid) and lower (dashed) than what is used for the best fit.

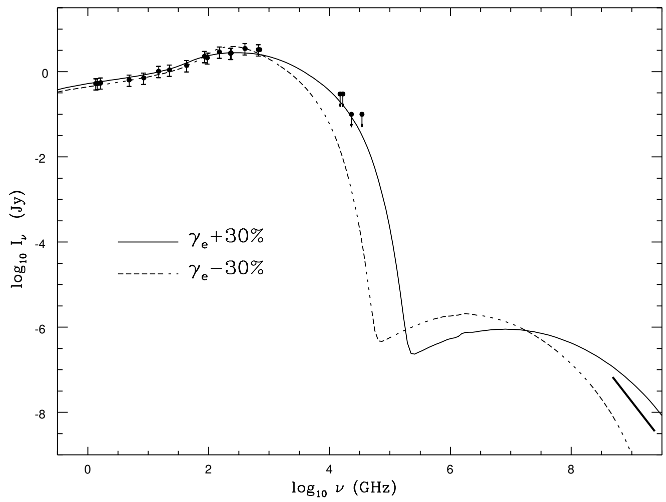

Fig. 3. Same as the power-law curve in Fig. 1, with the characteristic electron Lorentz factor plotted for values 30% higher (solid) and lower (dashed) than what is used for the best fit.

of the synchrotron emission being up-scattered. Hence, in order to produce soft X-ray emission from 1 THz synchrotron emission one needs $\gamma_{\rm e,0} \sim 100$. It is interesting to note that the characteristic $\gamma_{\rm e,0}$ (either the cut-off, for the power-law, or the peak, for the Maxwellian), discussed above in Sect. 3.1, required to both fit the correct radio emission from the nozzle while satisfying the IR upper limits falls exactly in this range.

To show how sensitive the model is to changes in parameters we display the same version of the power-law model with the crucial fit parameters B_0 and $\gamma_{\rm e,0}$ varied by 30% (Figs. 2 & 3). Changes in the magnetic field mainly reflect a change in the total flux level while changes in the electron energy most strongly affect the IR and X-ray emission. The Chandra detection therefore limits the $\gamma_{\rm e,0} \lesssim 130$, depending on the electron distribution. Attempting to fit both the radio and X-rays while remaining under the IR limits specifies a relatively tight range in parameters.

However, it is not completely clear if the Chandra X-rays originate in the jets or the accretion flow. The lower flux compared to that reported by ROSAT ($1-2\cdot 10^{34}$ erg s^{-1} within 0.8–2.5 keV, see Predehl & Zinnecker 1996) suggests that SSC could be an important component, however, thermal bremsstrahlung from the accretion flow may still play an important role even though the spectrum appears too steep at present. The true test will be comparing the predictions of the jet SSC component to future observations. These predictions are quite clear: we would expect significant, variable emission in the EUV to X-ray band, with the variability correlated with the already observed fluctuations in the submm-bump. The timescale for variations in the radio are between two weeks and several months (e.g., Falcke 1999b). Typical strong but perhaps infrequent flares in the mm-range seem to have timescales of about 20 days (Zhao et al., 2001; Tsuboi et al., 1999). Similar timescales are expected for the X-rays.

We also expect some curvature in the X-ray slope, rather than a pure power-law. Even if a mixture of jet SSC and emission from the hot accretion flow account for the X-ray flux of Sgr A*, the nozzle should still reveal itself through the correlated (with the radio) soft X-ray emission. Complete absence of X-ray variability would argue against SSC emission giving a major contribution.

If we do not attempt to account for the X-rays via SSC, the model is significantly less constrained, allowing for a larger range in the X-ray output (as long as it is under the Chandra limits) and thus in several of the parameters. This could later be fitted to a value if the assumedly (in this case) dominant disk and extended gas contribution is specified. However, if the Chandra flux proves to be variable in correlation with the radio, then the SSC component is a likely solution.

3.3. VLBI Size and Extended Emission

Possibly the most important constraints for any model are the VLBI measurements of the size of Sgr A*. Since most models have a stratified structure, the size of Sgr A* is expected to be a function of frequency. In our model, for a given observing frequency, the emission is highly concentrated to one spatial scale and thus predicts very little extended emission beyond the core (which is basically the $\tau = 1$ surface of the radio jet). The emission from the jets at a particular frequency is self-absorbed at small distances from the origin and cut off at large distances where the decreased magnetic field shifts the synchrotron cut-off frequency below the observing frequency. Thus, extended emission from the most visible jet is highly suppressed and the size of the detectable core will be a power-law $z \propto \nu^{-m}$ with $m \sim 0.9-1$. This also implies a shift of the location of the core with frequency.

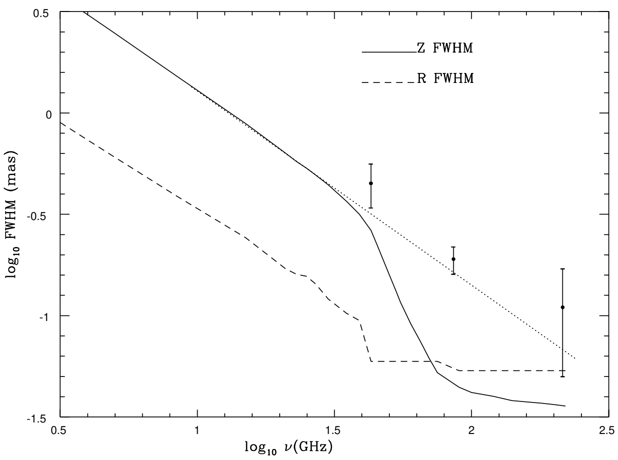

Fig. 4. Projected FWHM of the major and minor axis of the dominant jet as a function of frequency. The filled dots mark the FWHM as measured by Lo et al. (1998; 43 GHz) and Krichbaum et al. (1998; 86 & 215 GHz). At frequencies above 30 GHz one obtains a two component structure with an increasingly stronger core (nozzle, solid dashed line) and a fainter jet component (dotted line).

Fig. 4 compares the projected full width at half maximum (FWHM) of major and minor axis of the emission predicted by the jet model (for the jet pointing towards us) together with the upper limits imposed by high-frequency VLBI observations. Given the calibration difficulties (see discussion in Bower et al. 1999b), the values plotted can also be considered as upper limits on the source size in *one* direction (measurements at 3 and 1.4 mm wavelengths cover only a very restricted range in the (u,v)-space – see Doeleman et al. 1999 for a nice discussion of this problem).

Throughout the cm-wave range the predicted emission basically resembles one elliptical component decreasing in size with wavelength and only at mm-waves (i.e. above 30 GHz) does the more compact core-component, the nozzle, appear together with the more extended jet-emission. Comparing data and model in Fig.4 shows the extended jet emission is within the constraints imposed by VLBI—component ejections or a faint counter-jet could always make the jet somewhat larger. The exact size is also a function of the current flux density of Sgr A* and hence should vary on the same timescales found in the spectrum (see Falcke & Biermann 1999 for an analytic estimate of the functional dependence).

4. Discussion and Summary

We have calculated the emission expected from a jet model in the context of the Galactic Center. The spectrum of Sgr A*, including the new X-ray observations from Chandra, can be modeled entirely by emission from this jet. We can also show that the radio emission satisfies all constraints imposed by VLBI observations. This indicates that the basic jet model introduced by Falcke et al. (1993) can provide a detailed explanation of the Sgr A* radio and X-ray spectrum.

An important feature of the model is the highly peaked electron distribution (see also Beckert & Duschl 1997) which has a number of interesting implications:

a) In typical AGN core-jet sources the extended jet structure is due to an optically thin power-law. Here this extended emission is greatly suppressed due to the steep cut-off in the electron spectrum, required by the IR limits. This naturally can explain the compact jet structure as seen by Lo et al. (1998).
b) The X-ray emission produced via up-scattering of the synchrotron photons (SSC) can have a rather steep spectrum which is not a perfect power-law. This can well explain the very soft emission found for Sgr A* and perhaps also for M31* (Garcia et al., 2000) that otherwise seems to be too steep for thermal emission from accretion flows.
c) The nature of this distribution with $\gamma_{\rm e} \lesssim 100$ requires a closer look. The characteristic energy derived here for the electrons (or positrons) could be indicative of hadronic processes as discussed in Falcke (1996b), Mahadevan (1998), and Markoff et al. (2000).
d) Finally, in light of recent puzzling polarization measurements (Bower et al., 1999a; Bower et al., 1999b; Bower et al., 1999d), one needs to reconsider the polarization properties of synchrotron sources with such unusual electron distributions.

Our primary assumption is the existence of a nozzle close to the central black hole, which collimates a relativistic plasma having equipartition between the magnetic field and particles. The requirement that this nozzle is responsible for the dominant submm-bump in the radio, and possibly the SSC X-ray emission, allows us to fix most free parameters. Once the parameters for the nozzle are fixed by fitting the submm-bump, the evolution of magnetic field and density along the jet does not require additional parameters. The spectra we obtain are therefore generic for collimated outflows from any accretion flow—whether a magneto-hydrodynamical jet from a standard accretion disk or an outflow from an ADAF—provided the accretion flow can produce the required magnetic field, electron temperature, and density near its inner edge. For an ADAF or Bondi-Hoyle type accretion, the inclusion of jets near the black hole could thus enhance those models in accounting for the cm-wave radio emission. The energy requirements to produce such jets (see Falcke & Biermann 1999) are rather small compared to the power available through accretion of nearby winds (Coker and Melia, 1997). Therefore, it is possible that most of the visible emission in Sgr A* could be produced by an AGN-like jet and not an accretion flow.

Because the model is so generic, it is possible that this model finds an application also in other low-luminosity

AGN or even X-ray binaries. Here it needs to be checked whether in some cases similarly peaked electron distributions are present and whether some soft X-ray emission could be related to SSC emission from the jet.

Acknowledgements. We thank Mark Morris and Frederick K. Baganoff for providing us with information about the Chandra observations of Sgr A* before publication.

References

Backer, D. C. and Sramek, R. A., 1999, ApJ 524, 805
Baganoff, F. K., Angelini, L., Bautz, M., Brandt, N., Cui, W., Doty, J., Feigelson, E., Garmire, G., Kallman, T., Maeda, Y., Morris, M., Nishikida, K., Pravdo, S., Ricker, G., and Townsley, L., 1999, BAAS 195.6201
Baganoff, F. K., Maeda, Y., Morris, M., Bautz, M. W., Brandt, W. N., Cui, W., Doty, J. P., Feigelson, E. D., Garmire, G. P., Pravdo, S. H., Ricker, G. R., and Townsley, L. K., 2001, ApJ submitted
Beckert, T. and Duschl, W. J., 1997, A&A 328, 95
Bietenholz, M. F., Bartel, N., and Rupen, M. P., 2000, ApJ 532, 895
Blumenthal, G. R. and Gould, R. J., 1970, Reviews of Modern Physics 42, 237
Bower, G. C., Backer, D. C., Zhao, J. H., Goss, M., and Falcke, H., 1999a, ApJ 521, 582
Bower, G. C., Falcke, H., and Backer, D. C., 1999b, ApJ 523, L29
Bower, G. C., Falcke, H., Backer, D. C., and Wright, M., 1999c, in ASP Conf. Ser. 186: The Central Parsecs of the Galaxy, p. 80
Bower, G. C., Wright, M. C. H., Backer, D. C., and Falcke, H., 1999d, ApJ 527, 851
Coker, R. F. and Melia, F., 1997, ApJ 488, L149
Doeleman, S., Rogers, A. E. E., Backer, D. C., Wright, M., and Bower, G. C., 1999, in H. Falcke, A. Cotera, W. J. Duschl, F. Melia, and M.J. Rieke (eds.), ASP Conf. Ser. 186: The Central Parsecs of the Galaxy, p. 98, Astronomical Society of the Pacific, San Francisco
Eckart, A. and Genzel, R., 1996, Nature 383, 415
Falcke, H., 1996a, ApJ 464, L67
Falcke, H., 1996b, in IAU Symp. 169: Unsolved Problems of the Milky Way, Vol. 169, p. 169
Falcke, H., 1999a, in H. Falcke, A. Cotera, W. J. Duschl, F. Melia, and M.J. Rieke (eds.), ASP Conf. Ser. 186: The Central Parsecs of the Galaxy, p. 148, Astronomical Society of the Pacific, San Francisco
Falcke, H., 1999b, in H. Falcke, A. Cotera, W. J. Duschl, F. Melia, and M.J. Rieke (eds.), ASP Conf. Ser. 186: The Central Parsecs of the Galaxy, p. 113, Astronomical Society of the Pacific, San Francisco
Falcke, H. and Biermann, P. L., 1999, A&A 342, 49
Falcke, H., Goss, W. M., Matsuo, H., Teuben, P., Zhao, J. H., and Zylka, R., 1998, ApJ 499, 731
Falcke, H., Mannheim, K., and Biermann, P. L., 1993, A&A 278, L1
Falcke, H., Melia, F., and Agol, E., 2000a, ApJ 528, L13
Falcke, H., Nagar, N. M., Wilson, A. S., and Ulvestad, J. S., 2000b, ApJ 542, 197
Garcia, M. R., Murray, S. S., Primini, F. A., Forman, W. R., McClintock, J. E., and Jones, C., 2000, ApJ 537, 23
Ghez, A. M., Klein, B. L., Morris, M., and Becklin, E. E., 1998, ApJ 509, 678
Haller, J. W., Rieke, M. J., Rieke, G. H., Tamblyn, P., Close, L., and Melia, F., 1996, ApJ 468, 955
Herrnstein, J. R., Greenhill, L. J., Moran, J. M., Diamond, P. J., Inoue, M., Nakai, N., and Miyoshi, M., 1998, ApJ 497, L69
Krichbaum, T. P., Graham, D. A., Witzel, A., Greve, A., Wink, J. E., Grewing, M., Colomer, F., de Vicente, P., Gomez-Gonzalez, J., Baudry, A., and Zensus, J. A., 1998, A&A 335, L106
Lind, K. R. and Blandford, R. D., 1985, ApJ 295, 358
Lo, K. Y., Shen, Z. Q., Zhao, J. H., and Ho, P. T. P., 1998, ApJ 508, L61
Mahadevan, R., 1998, Nature 394, 651
Markoff, S., Falcke, H., and Biermann, P. L., 2000, in preparation
Melia, F., 1992, ApJ 387, L25
Nagar, N. M., Falcke, H., Wilson, A. S., and Ho, L. C., 2000, ApJ 542, 186
Narayan, R., Yi, I., and Mahadevan, R., 1995, Nature 374, 623
Özel, F., Psaltis, D., and Narayan, R., 2000, ApJ 541, 234
Predehl, P. and Trümper, J., 1994, A&A 290, L29
Predehl, P. and Zinnecker, H., 1996, in The Galactic Center, Vol. 102 of ASP Conf. Ser., p. 415, Astronomical Society of the Pacific, San Francisco
Rees, M. J., 1982, in AIP Conf. Proc. 83: The Galactic Center, pp 166–176
Reid, M. J., Readhead, A. C. S., Vermeulen, R. C., and Treuhaft, R. N., 1999, ApJ 524, 816
Reynolds, S. P. and McKee, C. F., 1980, ApJ 239, 893
Rogers, A. E. E., Doeleman, S., Wright, M. C. H., Bower, G. C., Backer, D. C., Padin, S., Philips, J. A., Emerson, D. T., Greenhill, L., Moran, J. M., and Kellermann, K. I., 1994, ApJ 434, L59
Serabyn, E., Carlstrom, J., Lay, O., Lis, D. C., Hunter, T. R., and Lacy, J. H., 1997, ApJ 490, L77
Tsuboi, M., Miyazaki, A., and Tsutsumi, T., 1999, in H. Falcke, A. Cotera, W. J. Duschl, F. Melia, and M.J. Rieke (eds.), ASP Conf. Ser. 186: The Central Parsecs of the Galaxy, p. 105, Astronomical Society of the Pacific, San Francisco
Wright, M. C. H. and Backer, D. C., 1993, ApJ 417, 560
Zhao, J.-H., Bower, G. C., and Goss, W. M., 2001, ApJ 547, 29